Available online at BCREC Website: http://bcrec.undip.ac.id

Bulletin of Chemical Reaction Engineering & Catalysis, 12 (1), 2017, 96-105

Research Article

Photocatalytic Degradation of Methyl Orange on Bi_2O_3 and Ag_2O-Bi_2O_3 Nano Photocatalysts

Seyed Ali Hosseini, Ramin Saeedi

Department of Chemistry, Faculty of Science, Urmia University, Urmia, Iran

Received: 15th August 2016; Revised: 20th December 2016; Accepted: 21st December 2016

Abstract

The photocatalytic activity of Bi_2O_3 and Ag_2O-Bi_2O_3 was evaluated by degradation of aqueous methyl orange as a model dye effluent. Bi_2O_3 was synthesized using chemical precipitation method. Structural analysis revealed that Bi_2O_3 contain a unique well-crystallized phase and the average crystallite size of 22.4 nm. The SEM analysis showed that the size of Bi_2O_3 particles was mainly in the range of 16-22 nm. The most important variables affecting the photocatalytic degradation of dyes, namely reaction time, initial pH and catalyst dosage were studied, and their optimal amounts were found at 60 min, 5.58 and 0.025 g, respectively. A good correlation was found between experimental and predicted responses, confirming the reliability of the model. Incorporation of Ag_2O in the structure of composite caused decreasing band gap and its response to visible light. Because a high percentage of sunlight is visible light, hence Ag_2O-Bi_2O_3 nano-composite could be used as an efficient visible light driven photocatalyst for degradation of dye effluents by sunlight.

Keywords: Ag_2O-Bi_2O_3 nano-composite; Photocatalyst; Bismuth nano-oxide; Dye degradation; Response surface methodology

How to Cite: Hosseini, S.A., Saeedi, R. (2017). Photocatalytic Degradation of Methyl Orange on Bi_2O_3 and Ag_2O-Bi_2O_3 Nano Photocatalysts. *Bulletin of Chemical Reaction Engineering & Catalysis*, 12 (1): 96-105 (doi:10.9767/bcrec.12.1.623.96-105)

Permalink/DOI: http://dx.doi.org/10.9767/bcrec.12.1.623.96-105

1. Introduction

Due to printing and dyeing industries, their wastewater as one of the industrial wastewaters is hard to treat because of its higher concentration, deep chromes, great toxicity and complicated component [1]. In particular, the pollution of water resources by organic pollutants, such as phenolic compounds, various dyes, etc., threatened the health of human beings [2]. Applications of the existing conventional physical-chemical and biological techniques represent unsatisfactory outcomes because of ineffective or nondestructive mineralization of these recalcitrant compounds [3]. Photocatalytic degradation of organic pollutant, such as RhB, a typical stable dyestuff, has been proved to be a viable environmentally benign technology to the decoloration and degradation of dye effluents [4]. In particular, nano-sized semiconductor particles with suitable surface areas and a variety of morphologies offer great opportunity [5]. Nanosized TiO_2 powders show extraordinarily high photocatalytic activities compared with commercial microsized powders [6].

The photocatalytic materials have mainly focused on TiO_2 semiconductor because of their high reactivity, low cost and environmentally

* Corresponding Author.
E-mail: s_ali_hosseini@yahoo.com (Hosseini, S.A.)

friendly features. Nevertheless, the TiO_2 needs UV light irradiation to produce the electronic transition responsible to its photo activity because of its large band gap of 3.2 eV [7]. Therefore, it is highly desirable to develop novel photocatalysts that can directly utilize visible light from sunlight. Among promising photocatalysts, bismuth-containing compounds show great application prospect. For example, Bi_2O_3 is an important metal oxide semiconductor with a direct band gap ranging from 2 to 3.9 eV and can be used to decompose dyes in wastewater under visible light UV and irradiation. By considering the energy and safety, photocatalysis under visible light is preferred rather UV irradiation. So, from this regards, Bi_2O_3 is preferred to TiO_2. Furthermore, Bi_2O_3 is rather inert in neutral water, which is a fundamental precondition for applications a photocatalyst for wastewater purification [8].

Bi_2O_3 has been prepared by solid-state reaction, sonochemical route, thermolysis, or hydrothermal treatment. The photo degradation of Rhodamine B, methyl orange, and peroxomonosulfate has been observed in the presence of Bi_2O_3 monoclinic [9]. For example, Qin *et al.* [10] prepared Bi_2O_3 and $(BiO)_2CO_3$ Nanotubes by a solvothermal method and evaluated their activities by photocatalytic degradation of RhB and Cr(VI) removal [10]. Pan and co-workers synthesized Bismuth Oxide Nanoparticles by a Templating method and tested its photocatalytic performance by decolorization of methyl orange solution under visible light condition [11].

The efficiency of a photocatalytic reaction depends on a number of factors, which govern the performance of photocatalysis. Initial concentration of pollutant, photocatalyst concentration, pH, volume of solution, radiant flux and agitation, irradiation time, light intensity, irradiation wavelength, temperature, geometrical parameters of the experimental setup and multiple degradation pathways are the parameters that can be cited. Due to the complexity and variety of influencing factors, it is difficult to evaluate the relative significance of several affecting factors, especially in the presence of complex interactions [12].

In this work, we tried to study the photocatalytic degradation of MO, by considering the effective factors on the degradation efficiency and modelling the process in order to get an insight to interactions of the process variable and importance of each variable on the degradation efficiency. The aim of this work is to synthesize Ag_2O-Bi_2O_3 nano-composite and to evaluate its photocatalytic performance in degradation of methyl orange (MO) by applying the response surface methodology (RSM). The RSM was used for design of experiment, modelling and optimization. The different variables, namely the amount of catalyst, initial pH, and reaction time were considered for the statistical study by RSM. The photocatalyst was characterized by XRD, FTIR and SEM.

2. Materials and Methods

2.1. Materials

Bismuth nitrate pentahydrate (100%), silver nitrate (≥99.8%), sodium hydroxide (99.9%), hydrochloric acid (37% by weight), nitric acid (65% by weight), and methyl orange (100%) all were purchased from Merck chemicals.

2.2. Synthesis of nano-Bi_2O_3

All materials were used without further purification. The nano-Bi_2O_3 was synthesized by precipitation method. First, a bismuth solution (0.2 $mol.L^{-1}$) was prepared by dissolution of $Bi(NO_3)_3.5H_2O$ in 1.5 $mol.L^{-1}$ nitric acid. Then concentrated sodium hydroxide was added drop by drop to above solution until pH 11.5. The white precipitates was appeared immediately and after several hours turned to yellow one. It was kept under magnetic stirring at room temperature for 24 h [9]. The collected precipitates were filtered, washed several times with distilled water and dried in an electric oven at 50 ^oC for 5 h.

2.3. Synthesis of Ag_2O-Bi_2O_3 nano-composite

Ag_2O-Bi_2O_3 composite with ion ratio (Ag^+: Bi^{3+}) 3:1 was synthesized using simple chemical precipitation method. A determined amount of Bi_2O_3 nano particle and 2 g PEG-8000 were added to 100 mL deionized water and stirred for 5 min. Then $Ag(NO_3)$ was added into above mixture and the pH was adjusted to 14 by dropwise addition of NaOH (4 M) solution under magnetic stirring for 10 min. the prepared composite was filtered, washed several times with water and dried at 90 ^oC for 2 h in an electric oven.

2.4. Characterizations of photocatalysts

The structure and phase characteristic of as-prepared Bi_2O_3 was determined by X-ray diffraction patterns [XRD, Philips X, pert diffractometer using Cu Kα radiation]. The data were recorded in the 4-60° 2θ range with 0.02°

steps. The morphology of sample, coated with gold, was examined using Scanning electron microscopy Tecsan (Mira 3). The absorption data of degraded aqueous solutions were collected using a UV-Vis spectrometer.

2.5. Photocatalytic tests

Photocatalytic activity of Ag_2O-Bi_2O_3 nanocomposite was evaluated by degradation of MO under simulated sunlight. A simulated sunlight irradiation (blended-mercury lamp, Noor, Iran) has been taken for visible light irradiation. For each experiment, determined amount of catalyst was suspended in 100 ml dye solution. Prior to illumination, the suspension was stirred continuously in the dark for 30 min to ensure the establishment of an adsorption between dye and surface of catalyst. Then the pH was adjusted using NaOH and HCl. Next, the solution was illuminated according to designed experiments. At the given intervals, 3 mL aliquots were taken out and centrifuged to remove the catalysts. Figure 1 shows a simple schematic diagram of experimentation. The samples were analyzed by UV-Vis spectroscopy. The degradation percentage, *D*, was calculated by Equation 1.

$$D\% = \frac{A_o - A_t}{A_p} x100 \quad (1)$$

where A_0 and A_t are the initial and final absorbance of dye, respectively.

2.6. Determination of the point of zero charge

The point of zero charge of Bismuthnanooxide was determined using mass titration (MT) method suggested by Noh and Schwarz [13]. Several aqueous suspensions containing various amount of the immersed Bi_2O_3 and 10 mL of NaCl (0.1 M) as electrolyte were prepared and agitated for 24 h in a shaker at 220 rpm to reach an equilibrium pH values. Then the curve pH versus sorbent mass was plotted. The plateau in the MT curve corresponds to pH_{pzc}.

2.7. Response surface methodology (RSM)

Response Surface Methodology (RSM) is a family of statistical techniques for the design, empirical modeling and optimization of processes, where the responses of interest are influenced by several process variables (termed factors). RSM comprises the following three major components: (i) experimental design to determine the values of process factors based on which experiments are conducted and data are collected; (ii) empirical modeling to approximate the relationship (i.e. the response surface) between responses and factors; (iii) optimization to find the best response value based on the empirical model. In addition, the above three stage procedure is typically operated in an iterative manner, where the information attained from previous iterations is utilized to guide the search for better response variables. RSM is particularly applicable to problems where the understanding of the process mechanism is limited and/or is difficult to be represented by a first-principles mathematical model. Depending on specific objectives in practice, these RSM techniques differ in the experimental design procedure, the choice of empirical models, and the mathematical formulation of the optimization problem [14]. The use of Box-Behnken design is popular in industrial research because it is an economical design and requires only three levels (-1, 0, 1) for each factor [15]. The most important factors, which affect the photocatalytic degradation of dye effluents in aqueous solution are catalyst amount, initial pH and reaction time. Therefore, the three variables were considered at a

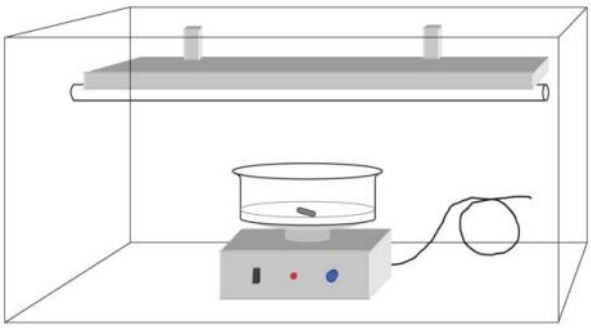

Figure 1. A simple schematic diagram of experimentation

Table 1. Independent variables and their levels for the Box-Behnken design used in the photocatalytic degradation of MO

Variable	Symbol	Uncoded Levels		
		Minimum (-1)	Mean (0)	Maximum (+1)
Catal. Amount (g)	X_1	0.025	0.05	0.075
Reaction time (min)	X_2	20	40	60
Initial pH	X_3	3	7	11

constant concentration of MO (10 ppm). The three independent variables were converted to dimensionless ones (X_1, X_2, X_3), with the uncoded values at the three levels. Values and limits of independent variables, determined by preliminary experiments, are shown in Table 1.

A total of 15 experiments for MO degradation consisting of three-factorial and three BBD levels were applied in the present work, including one replication at the center point. The complete experimental design matrix and the response based on experimental runs proposed by BBD for the photocatalytic degradation of MO are given in Table 2, respectively.

In the optimization process, BBD results were used for figuring, where Y is the selected response (dependent variable), X_1 to X_i are the independent variables being optimized. The calculation was aimed at predicting the better combination of independent variables for the optimization of the MO photocatalytic degradation conditions. Accordingly, the better combination of X_1 (amount of catalyst), X_2 (reaction time), X_3 (initial pH) for maximizing MO degradation were achieve by using the below second-order polynomial Equation 2.

$$Y = b_0 + \sum_{i=1}^{n} b_i X_i + \sum_{i=1}^{n} b_{ii} X_i^2 + \sum_{i=1}^{n-1} \sum_{j=i-1}^{n} b_{ij} X_i X_j \quad (2)$$

where Y presents the predicted response, b_0 is the constant coefficient, b_i the linear coefficients, b_{ij} the interaction coefficients, b_{ii} the quadratic coefficients and, X are the coded levels of the factors investigated. The coefficients of determination R^2 and R^2_{adj} expressed the quality of fit of the resultant polynomial model, and statistical significance was checked by F-test in the program. The desired goals in optimization were selected as maximum degradation of dye effluents (MO) at minimum catalyst amount, reaction time and optimum initial pH.

3. Results and Discussion

3.1. XRD pattern of nano-Bi_2O_3

The phase analysis and structure of as-prepared sample was studied using XRD pattern. Figure 2 shows the diffractograph of Bi_2O_3. The strong diffraction peaks reveal high crystallinity of as-synthesized sample. All peaks can be readily indexed to Bi_2O_3 with a monoclinic structure without any other impurity, which is in agreement with standard reference of JCPDS 41-1449 [16]. The average crystalline size of 22.4 nm was calculated using the Debye-Scherrer Equation 3.

Table 2. Experimental design matrix and responses based on experimental runs proposed by BBD design for MO degradation

Run	Independent Variables			Response (R)
	A	B	C	Experimental
	Catal. Amount (g)	Reaction time (min)	Initial pH	Degradation (%)
1	0.025	40	3	24.73
2	0.025	60	7	84.54
3	0.05	60	11	17.70
4	0.025	20	7	55.72
5	0.075	40	11	10.53
6	0.05	20	3	28.23
7	0.05	40	7	52.28
8	0.05	20	11	9.43
9	0.075	60	7	78.93
10	0.05	40	7	49.11
11	0.05	40	7	55.65
12	0.075	40	3	40.58
13	0.075	20	7	43.31
14	0.05	60	3	64.58
15	0.025	40	11	5.41

$$\overline{D} = \frac{0.89\lambda}{\beta \cos\theta} \quad (3)$$

3.2. FT-IR spectrum of nano-Bi_2O_3 and Ag_2O-Bi_2O_3 nano-composite

Figure 3 shows the FT-IR spectrum of Bi_2O_3 (red plot) and Ag_2O-Bi_2O_3 nano-composite (blue plot). In the case of the red plot, the broad peak at 3451 cm^{-1} is related to stretching vibration of hydrogen-banded surface water molecules and hydroxyl groups. The peak at 1628 cm^{-1} corresponds to the vibrating mode of residual hydroxyl groups. The band at 847 cm^{-1} implies the vibration of Bi–O bonds and existence of a Bi_2O_3. This analysis is consistent with reported literatures [17]. As it clear from the blue plot, all peaks are similar to pure Bi_2O_3 peaks expect the peak at 542 cm^{-1} which corresponds to vibrational mode of Ag–O bond.

3.3. SEM images of nano-Bi_2O_3

The morphology of precursor was investigated by emission-scanning electron microscopy. Figure 4 shows FESEM images of Bi_2O_3 prepared by chemical precipitation method. FESEM images indicate that the precursor predominantly consists of nearly spherical particles in the range 15.39-21.37 nm.

3.4. Data analysis and evaluation of the model by RSM

A semi-empirical model for photocatalytic degradation of MO by Ag_2O-Bi_2O_3 nano-composite was developed through data analysis by means of Minitab 16 software. Equation 4 expressed the second-order polynomial model Y is the degradation percentage of MO.

$$Y = 53.6 + 0.37X_1 + 13.63X_2 - 14.38X_3 + 11.34X_2^2 - 33.98X_3^2 - 2.68X_1X_3 - 7.2X_2X_3 \quad (4)$$

In the model (Equation (4)), X_1 to X_3 correspond to the independent variables of the amount of catalyst (Ag_2O-Bi_2O_3), reaction time, and initial pH, respectively.

The correlation between experimental data and responses predicted by the model were evaluated. The model explains perfectly the studied experimental range (R^2_{MO} = 0.9624). This fact is clear in Figure 5 by comparing the experimental values against the predicted responses by the model for the percentage of MO degradation, respectively. Table 3 shows the analysis of variance (ANOVA) results for MO degradation. In order to have a significant term at this confidence level, the calculated probability should be lower than 0.05. Therefore, the value of probability bigger than F-value (i.e. the probability for the F-value to be higher than the calculated F-value in the table to accept null hypothesis) for all terms (X_1, X_2, X_3) which is less than 0.05, indicates that these model terms are statistically significant.

3.5. Standardized Pareto Chart

The importance of the calculated factors in the model was evaluated. Figure 6 presents the single factor and interactions of factors depicted in rank order in the form of Pareto Chart for MO. All factors were in absolute values and surpass the vertical significance line

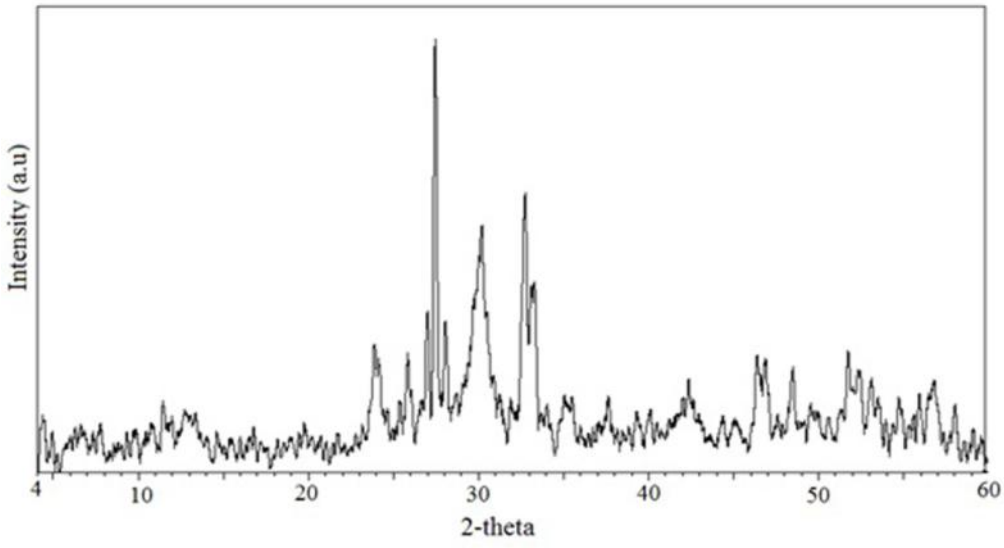

Figure 2. XRD pattern of Bi_2O_3

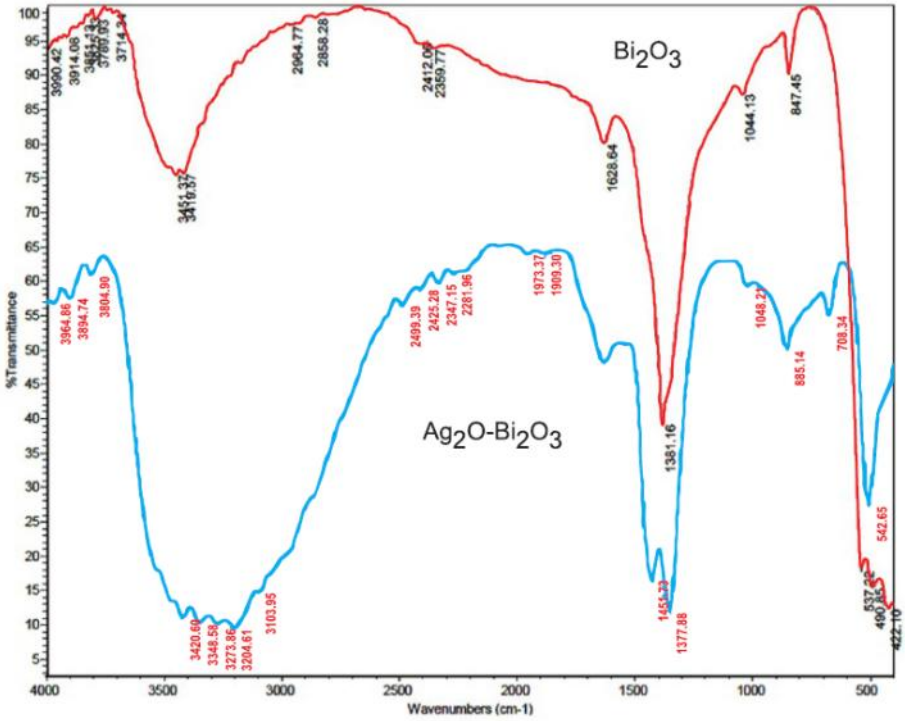

Figure 3. FTIR spectrum of Bi_2O_3 and Ag_2O-Bi_2O_3 nano-composite

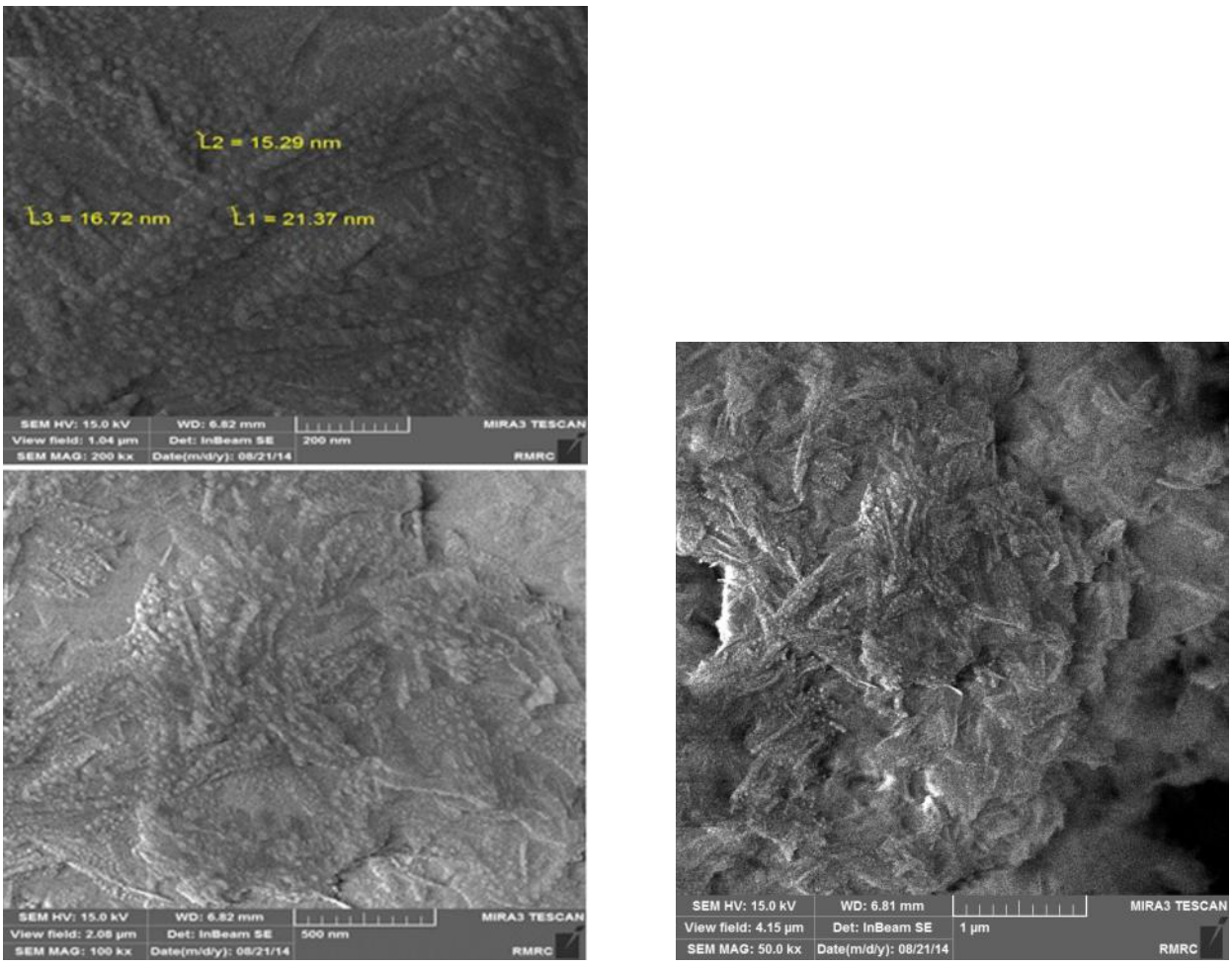

Figure 4. FESEM images of nano-Bi_2O_3

(95 confidence intervals) which exerted a statistically significant influence on the response. It is observed that the factor interactions and single factors are important parameters for MO degradation.

The Pareto chart (Figure 6) suggests that among selected variables for degradation of MO by Ag_2O-Bi_2O_3 nano-composite, X_3X_3 (initial pH-initial pH) and X_3 (initial pH) have the main effect on degradation efficiency.

3.6. Effects of operational parameters on photocatalytic degradation of MO

Fitted response surface for MO removal was achieved from Equation (4) using Minitab 16 software and it is illustrated in Figure 7 (a-b). Figure 7(a) shows the effect of initial pH and irradiation time on photocatalytic degradation of MO as the response surface and contour lines plot for catalyst amount 0.05 g. It is obvious from Figure 7(a), increasing the initial pH from acidic media to neutral increased the degradation efficiency of MO, but more increasing pH resulted in reducing degradation efficiency. According to Pareto analysis, the pH of MO solution plays a prominent role on photocatalytic activity of Ag_2O-Bi_2O_3. The change of pH influences not only the molecular speciation of MO in aqueous solution, but also the surface charge state of catalyst. The dissociation constant pKa for MO is 3.46 [18], therefore MO ions were predominantly present as monovalent anions at these equilibrium pHs. In alkaline pHs, because of electrostatic repulsion between MO anions and the negative charged surface of photocatalyst, the photocatalytic removal of MO is low. Moreover, the hydroxyl groups on the surface of prepared catalysts act as an electron donor for photo-generated H^+, and form active hydroxyl radicals (•OH) which attack the dye [19], but there is a Coulombic repulsion between the negative charged surface of photocatalyst and the hydroxide anions. This fact could prevent the formation of •OH and thus decrease the photoxidation [20]. Therefore, de-

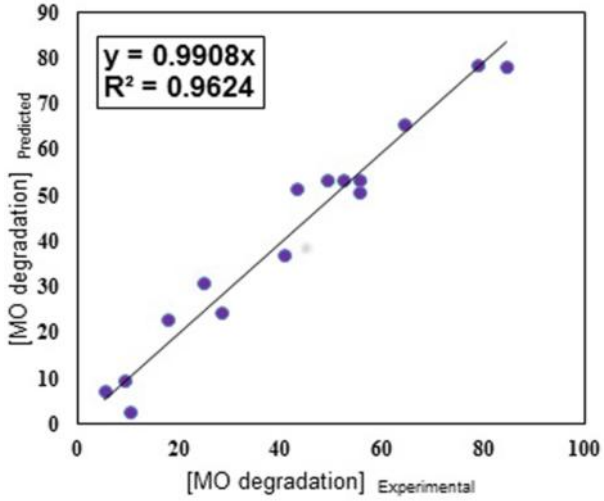

Figure 5. Comparison between the experimental values of MO degradation and those calculated by using the second-order polynomial Equation (3) reported in the text (predicted values)

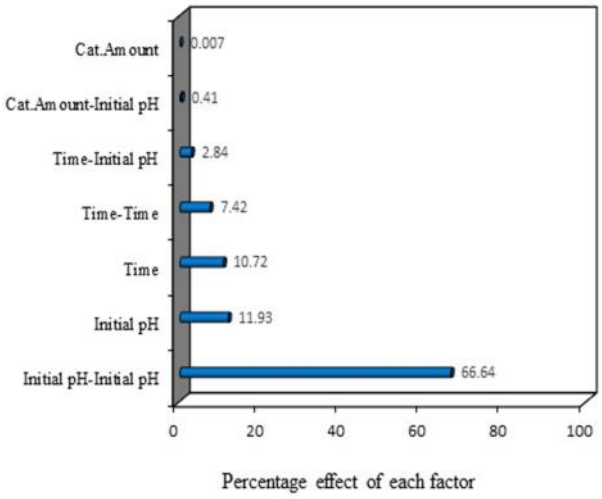

Figure 6. Standardized effects of single and interaction factors on photocatalytic degradation of MO

Table 3. Analysis of variance (ANOVA) for optimization of photocatalytic degradation of MO

Response	Source	Degrees of freedom	Sum of square	Mean square	F
MO degradation	Regression	7	8363.14	1194.73	26.35
	Residual error	7	317.34	45.33	
	total	14	8680.48		

$R^2 = 0.9624$, $R^2_{adj} = 0.9269$

colorization efficiency was observed to be low at basic pH. Similar results have been reported for the effect of pH on photocatalytic degradation of dye effluents [21,22]. It is also evident from figure, degradation efficiency increased with increasing irradiation time and at least 75% MO was degraded after irradiation time of 57 min.

Figure 7(b) illustrates the response surface and contour lines plot for degradation efficiency as a function of catalyst amount and irradiation time at initial pH = 7. As it is clear from this figure, degradation efficiency relatively was constant with increasing catalyst amount (Ag_2O-Bi_2O_3). The reason of this observation is thought to be the fact that when all dye molecules are adsorbed on the catalyst, the addition of higher quantities of the catalyst would have no effect on the degradation efficiency [23]. However, its effect on degradation of MO is less significant.

3.7. Effect of Ag_2O on photocatalytic property of nano-composite (Ag_2O-Bi_2O_3)

The energy band structure feature of a semiconductor greatly determines the efficiency of photocatalytic activity. In order to adjust the band gap and absorb visible light in a wider range, combining two kinds of semiconductor photocatalysts is a promising way. Ag_2O with a band gap of 1.3 eV shows strong absorption of both UV and visible light [24]. Hence, the existence of Ag_2O in nano-composite structure can increase the visible light absorption range of the composite photocatalyst, as reported in literature [25,26]. The band gap of Bi_2O_3 is about 2.82 eV, while the band gap of Ag_2O-Bi_2O_3 is 2.30 [24] that shows an obvious decrease. Decreasing the band gap of nano-composite (Ag_2O-Bi_2O_3) results in response to visible light.

3.8. Process optimization using response surface methodology

The last step of the RSM is to obtain the optimal conditions for the photocatalytic degradation of MO over nanophotocatalysts. The optimal conditions in MO degradation by Ag_2O-Bi_2O_3 nano-composite were found at 0.025 g (catalyst amount), 60 min (irradiation time) and 5.58 (initial pH). The optimal experiment predicted by modeling was experimentally carried out, in order to further assess the validity of model. The response of experiment for MO

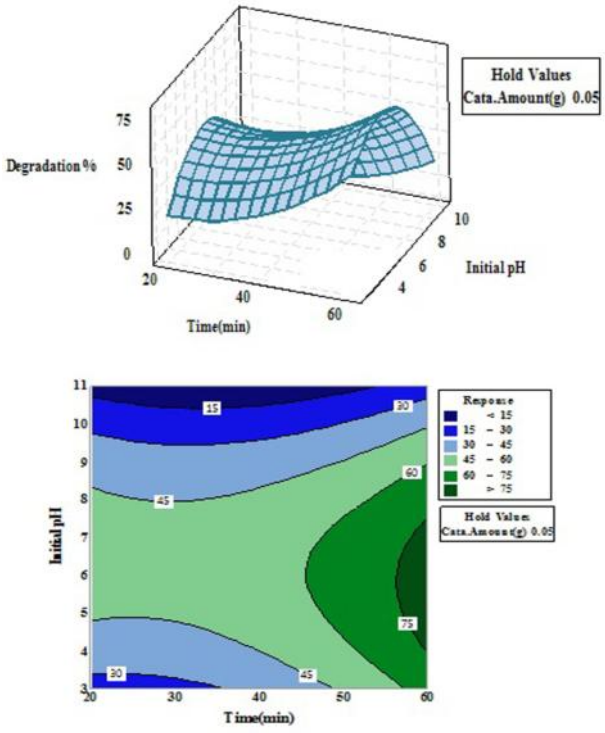

Figure 7(a). Response surface and contour-lines plots for initial pH and irradiation time (min), holding the other variable at its center level, catalyst amount 0.05 g

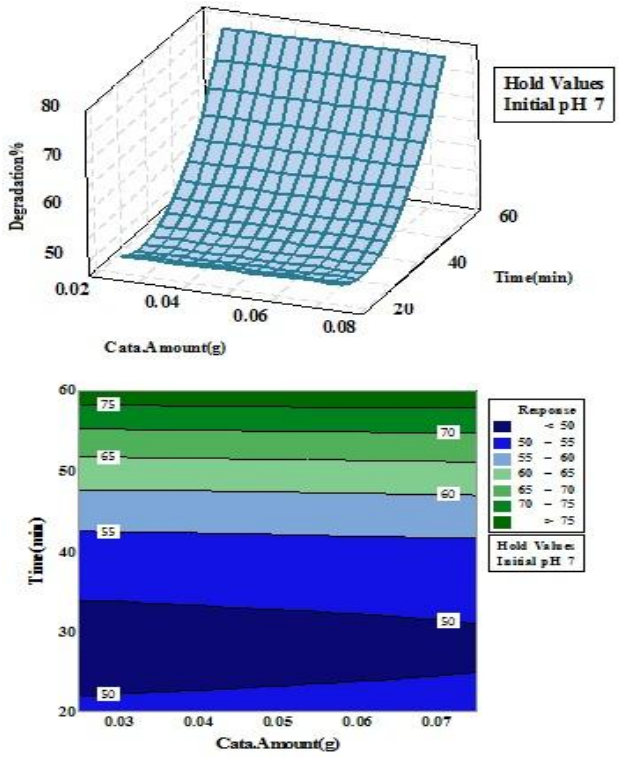

Figure 7(b). Response surface and contour-lines plots for catalyst amount and irradiation time (min), holding the other variable at its center level, initial pH=7

degradation was the same as the range predicted by the model. Consequently, the validity and adequacy of the model were verified.

4. Conclusions

The photocatalytic activity of Bi_2O_3 and Ag_2O-Bi_2O_3 nano-composite for degradation of dye pollutants was successfully investigated. The Ag_2O-Bi_2O_3 nano-composite exhibited activity for degradation of MO under visible light. The modeling of the photocatalytic processes and interaction between significant factors in both degradation processes was studied by RSM. Analysis of variance demonstrated a high determination coefficient between experimental data and predicted values by the developed models, indicating that the second-order polynomial order could be applied for optimization process. The photocatalytic process was observed above the PZC of Bi_2O_3. It was also resulted that in alkaline condition, photocatalytic degradation of dyes is negligible. The Ag_2O-Bi_2O_3 nano-composite presents a high photocatalytic activity under simulated sunlight, hence it can be a good candidate for degradation dye effluents without secondary pollution.

Acknowledgement

Especially thank Iranian Nanotechnology Initiative Council for financial supports.

References

[1] Chen, L., Zhang, S., Wang, L., Xue, D., Yin, S. (2009). Photocatalytic Activity of Zr: $SrTiO_3$ under UV Illumination. *J. Crystal Growth*, 311: 735-737.

[2] Hu, R., Li, C., Wang, X., Zhou, T., Yang, X., Gao, G., Zhang, Y. (2013). Synthesis of Perovskite $KMgF_3$ with Microemulsion for Photocatalytic Removal of Various Pollutants under Visible Light. *Catal. Commun.*, 40: 71-75.

[3] Su, M., He, C.K., Sharm, V., AbouAsi, M., Xia, D., Li, X.Z., Deng, H., Xiong, Y. (2012). Mesoporous Zinc Ferrite: Synthesis, Characterization, and Photocatalytic Activity with H_2O_2/Visible Light. *J. Hazard Mater.*, 211-212: 95-103.

[4] Ding, J., Lü, X., Shu, H., Xie, J., Zhang, H. (2010). Microwave-Assisted Synthesis of Perovskite $ReFeO_3$ (Re: La, Sm, Eu, Gd) Photocatalyst. *Mater. Sci. Eng. B*, 171: 31-34.

[5] Han, L., Zhou, X., Wan, L., Deng, Y., Zhan, S. (2014). Synthesis of $ZnFe_2O_4$ Nanoplates by Succinic Acid-Assisted Hydrothermal Route and their Photocatalytic Degradation of Rhodamine B under Visible Light. *J. Environ. Chem. Eng.*, 2: 123-130.

[6] Peng, C., Gao, L. (2008). Optical and Photocatalytic Properties of Spinel $ZnCr_2O_4$ Nanoparticles Synthesized by a Hydrothermal Route. *J. Am. Ceram. Soc.*, 91: 2388-2390.

[7] Belver, C., Ada´n, C., Ferna´ndez-Garcı´a, M. (2009). Photocatalytic Behavior of Bi_2MO_6 Polymetalates for Rhodamine B Degradation. *Catal. Today*, 143: 274-281.

[8] Liu, X., Cao, H., Yin, J. (2011). Generation and Photocatalytic Activities of Bi@Bi_2O_3 Microspheres. *Nano Res.*, 4(5): 470-482.

[9] Saison, T., Chemin, N., Chaneac, C., Durupthy, O., Ruaux, V., Mariey, L., Mauge, F., Beaunier, P., Jolivet, J.P. (2011). Bi_2O_3, $BiVO_4$, and Bi_2WO_6: Impact of Surface Properties on Photocatalytic Activity under Visible Light. *J. Phys. Chem. C*, 115: 5657-5666.

[10] Qin, F., Li, G., Wang, R., Wu, J., Sun, H., Chen, R. (2012). Template-Free Fabrication of Bi_2O_3 and $(BiO)_2CO_3$ Nanotubes and their Application in Water Treatment. *Chem. Eur. J.*, 18: 16491-16497.

[11] Pan, C., Yan, Y., Li, H., Hu, S. (2012). Synthesis of Bismuth Oxide Nanoparticles by a Templating Method and Its Photocatalytic Performance. *Adv. Mater. Res.*, 557-559: 615-618.

[12] Khataee, A.R., Kasiriand, M.B., Alidokht, L. (2011). Application of Response Surface Methodology in the Optimization of Photocatalytic Removal of Environmental Pollutants using Nanocatalysts. *Environ. Technol.*, 32:1669-1684.

[13] Subramanian, S., Noh, J.S., Schwarz, J.A. (1988). Determination of the Point of Zero Charge of Composite Oxides. *J. Catal.*, 114: 433-439.

[14] Salari, D., Niaei, A., Aghazadeh, F., Hosseini, S.A., Seyednajafi, F. (2012). Catalytic Remediation of 2-Propanol on Pt-Mn/γ-Al_2O_3 Bimetallic Catalyst during Catalytic Combustion-Experimental Study and Response Surface Methodology (RSM) Modeling. *J Environ. Sci. Health Pt A*, 47: 351-357.

[15] Khuri, I.A., Mukhopadhyay, S. (2010). Response Surface Methodology. *WIREs Comp. Stat.*, 2: 128-149.

[16] Rivenet, M., Roussel, P., Abraham, F. (2008). One-Dimensional Inorganic Arrangement in The Bismuth Oxalate Hydroxide $Bi(C_2O_4)OH$. *J. Solid State Chem.*, 181: 2586-2590.

[17] Ma, M.G., Zhu, J.F., Sun, R.C., Zhu, Y.J. (2010). Microwave-Assisted Synthesis of Hierarchical Bi_2O_3 Spheres Assembled from

Nanosheets with Pore Structure. *Mater. Lett.*, 64: 1524-1527.

[18] Zaghouane-Boudiaf, H., Boutahala, M., Arab, L. (2012). Removal of Methyl Orange from Aqueous Solution by Uncalcined and Calcined MgNiAl Layered Double Hydroxides (LDHs). *Chem. Eng. J.*, 187: 142-149.

[19] Pouretedal, H.R., Ahmadi, M. (2013). Preparation, Characterization and Determination of Photocatalytic Activity of MCM-41/ZnO and MCM-48/ZnO Nanocomposites. *Iranian J. Catal.*, 3(3): 149-155.

[20] Akpan, U.G., Hameed, B.H. (2009). Parameters Affecting the Photocatalytic Degradation of Dyes using TiO_2-based Photocatalysts: A Review. *J. Hazard Mater.*, 170: 520-529.

[21] Daneshvar, N., Salari, D., Khataee, A.R. (2004). Photocatalytic Degradation of Azo Dye Acid Red 14 in Water on ZnO as an Alternative Catalyst to TiO_2. *J. Photochem. Photobiol. A*, 162: 317-322.

[22] Cho, H., Zoh, K.D. (2007). Photocatalytic Degradation of Azo Dye (Reactive Red 120) in TiO_2/UV System: Optimization and Modeling using a Response Surface Methodology (RSM) Based on the Central Composite Design. *Dyes Pigm.*, 75: 533-543.

[23] Daneshvar, N., Salari, D., Khataee, A.R. (2003). Photocatalytic Degradation of Azo Dye Acid Red 14 in Water: Investigation of the Effect of Operational Parameters. *J. Photochem. Photobiol. A*, 157: 111-116.

[24] Zhu, L., Wei, B., Xu, L., Lu, Z., Zhang, H., Gao, H., Che, J. (2012). Ag_2O-Bi_2O_3 Composites: Synthesis, Characterization and High Efficient Photocatalytic Activities. *Cryst. Eng. Comm.*, 14: 5705-5709.

[25] Zhang, L., Wang, W., Yang, J., Chen, Z., Zhang, W., Zhou, L., Liu, S. (2006). Sonochemical Synthesis of Nanocrystallite Bi_2O_3 as a Visible-Light-Driven Photocatalyst. *Appl. Catal. A: Gen.*, 308: 105-110.

[26] Muruganandham, M., Amutha, R., Lee, G.J., Hsieh, S.H., Wu, J., Sillanpaa, M. (2012). Facile Fabrication of Tunable Bi_2O_3 Self-Assembly and Its Visible Light Photocatalytic Activity. *J. Phys. Chem. C*, 116: 12906-12915.